Journal of Power Sources 249 (2014) 277–284

Contents lists available at ScienceDirect

Journal of Power Sources

journal homepage: www.elsevier.com/locate/jpowsour

H_3PO_4 imbibed polyacrylamide-graft-chitosan frameworks for high-temperature proton exchange membranes

Shuangshuang Yuan [a], Qunwei Tang [a,*], Benlin He [a], Haiyan Chen [a], Qinghua Li [b], Chunqing Ma [a], Suyue Jin [a], Zhichao Liu [a]

[a] Institute of Materials Science and Engineering, Ocean University of China, Qingdao 266100, Shandong Province, PR China
[b] National Defense Key Disciplines Laboratory of Light Alloy Processing Science and Technology, Nanchang Hangkong University, Nanchang 330063, PR China

HIGHLIGHTS

- H_3PO_4 is imbibed into 3D framework of PAAm-graft-chitosan hydrogel.
- The proton conductivity can be controlled by adjusting NMBA dosage.
- An anhydrous proton of 0.13 S cm^{-1} at 165 °C is obtained.
- The promising hydrogel-matrix membranes can be potentially used in PEMFCs.

ARTICLE INFO

Article history:
Received 23 September 2013
Received in revised form
22 October 2013
Accepted 23 October 2013
Available online 4 November 2013

Keywords:
Proton exchange membrane
Hydrogels
Proton conductivity
Fuel cells

ABSTRACT

Proton exchange membrane (PEM), transferring protons from anode to cathode, is a key component in a PEM fuel cell. In the current work, a new class of PEMs are synthesized benefiting from the imbibition behavior of three-dimensional (3D) polyacrylamide-graft-chitosan (PAAm-graft-chitosan) frameworks to H_3PO_4 aqueous solution. Interconnected 3D framework of PAAm-graft-chitosan provides tremendous space for holding proton-conducting H_3PO_4. The highest anhydrous proton conductivity of 0.13 S cm^{-1} at 165 °C is obtained. A fuel cell using a thick membrane as a PEM showed a peak power density of 405 mW cm^{-2} with O_2 and H_2 as the oxidant and fuel, respectively. Results indicate that the interconnected 3D framework provides superhighway for proton conduction. The valued merits on anhydrous proton conductivity, huge H_3PO_4 loading, and easy synthesis promise the new membranes to be good alternatives as high-temperature PEMs.

1. Introduction

Proton exchange membrane fuel cells (PEMFCs) are promising solution to energy depletion, environmental pollution, and ecological destruction [1,2]. It is honored as an electrochemical device converting chemical energy into electric energy characterized by a high efficiency. As a core component, proton exchange membrane (PEM) is a medium transferring protons from anode to cathode [3,4]. There is a high dependence of fuel cell performances on kinetics of transferring protons. The representative of the first-generation PEMs is Nafion [5], a sulfonated tetrafluoroethylene based fluoropolymer-copolymer discovered in the late 1960s by Walther Grot of DuPont. Nafion has received a considerable amount of attention as a proton conductor for PEMFCs on behalf of its excellent thermal and mechanical stabilities. The main problem of Nafion membranes is their high cost, therefore, sulfonation of engineering polymers have been developed to replace Nafion [6–8]. No matter Nafion or sulfonated engineering polymers, an insurmountable issue is the participation of water in transferring protons benefiting from the dissociation of sulfonic acid group in water atmosphere, which results in a fussy water-supplying equipment and low-temperature operation (<100 °C) [9]. The associated problems of low-temperature PEMFCs are Pt poisoning, high Pt dosage, and low reaction kinetics in anode, cathode as well as PEM. One efficient route of overcoming these problems is to elevate the operating temperature of PEMFCs to 100–180 °C. At so high temperatures, the CO molecules cannot bond onto the active sites of Nano-Pt electrocatalyst on behalf of the increased molecular dynamics [10,11]. The release of abundant active sites of Pt catalysts can generate high electrode kinetics.

* Corresponding author. Tel./fax: +86 532 66781690.
E-mail address: tangqunwei@hotmail.com (Q. Tang).

0378-7753/$ – see front matter © 2013 Elsevier B.V. All rights reserved.
http://dx.doi.org/10.1016/j.jpowsour.2013.10.104

In a high-temperature PEMFC, H_3PO_4 is always employed as an anhydrous proton conductor and linear polybenzimidazole (PBI) is a matrix. However, the protonation of PBI by H_3PO_4 always results in a low H_3PO_4 loading and therefore low proton conductivity [12]. Moreover, the H_3PO_4 doped PBI membranes suffer from attack of water generated in cathode because of linear nature of PBI backbone. In search for new class of high-temperature PEMs, Tang et al. pioneerly proposed the concept of employing extraordinary "imbibition" and large capacity of hydrophilic hydrogels to H_3PO_4 aqueous solution or hydrophobic hydrogels to H_3PO_4 alcohol solution, forming anhydrous hydrogel-matrix high-temperature PEMs during dehydration process [13–17]. "Hydrogels" are a category of weakly crosslinked three-dimensional (3D) polymer frameworks decorated with plenty of hydrophilic groups (−COOH, $-COO^-$, $-CONH_2$, $-SO_3H$, or −OH), by which more than 99 wt% of aqueous solution in mass can be imbibed with no leakage [18–20]. There is a consensus that non-ionic hydrogels, such as polyacrylamide (PAAm), have better imbibition capacity to H_3PO_4 aqueous solution than that of ionic hydrogels (such as polyacrylate). The combination of PAAm with natural macromolecules is considered as a facile route of further enhancing imbibition capacity [21].

Here we report the fabrication of PAAm-graft-chitosan and employment as H_3PO_4 placeholder. The 3D framework is adjusted by changing synthesis conditions to optimize H_3PO_4 loading and therefore proton conductivity. The focus of current work is to investigate the dependence of electrical and electrochemical behaviors of H_3PO_4 imbibed PAAm-graft-chitosan high-temperature PEMs on crosslinker dosage and preliminary fuel cell performances.

2. Experimental

2.1. Synthesis of PAAm-graft-chitosan membranes

The PAAm-graft-chitosan membranes were synthesized by modifying the procedures in previous literature [13–17]: In details, a solution mixture consisting of acrylamide monomer (10 g, AAm, analytical reagent) and chitosan (0.3 g, analytical reagent) was made by agitating in 10 mL of deionized water in a water-bath at 80 °C. Under vigorous agitation, crosslinker *N*,*N*′-(methylene) bisacrylamide (NMBA, 0.002–0.01 g) and initiator ammonium persulfate (APS, 0.045 g) were subsequently added to the above mixture. With proceeding of polymerization, the viscosity increased gradually. When the viscosity of the PAAm-graft-chitosan reached around 180 mPa s^{-1}, the reagent was poured into a Petri dish and cooled to room temperature with the formation of an elastic transparent gel. The PAAm-graft-chitosan membranes were then molded into φ 2.5 cm die. After rinsing with deionized water, the membranes were dried under vacuum at 60 °C for 24 h.

2.2. Preparation of H_3PO_4 imbibed PAAm-graft-chitosan membranes

The dried PAAm-graft-chitosan membranes were immersed in H_3PO_4 aqueous solution with concentration varying from 0.1 to 11 M in a sealed bottle at room temperature for 20 days to reach absorption equilibrium. The resultant products were then filtered and dried under vacuum at 60 °C for 2 days to drive off all water and obtain the anhydrous H_3PO_4 imbibed PAAm-graft-chitosan membranes. H_3PO_4 loading (wt%) was determined by measured according to Equation (1):

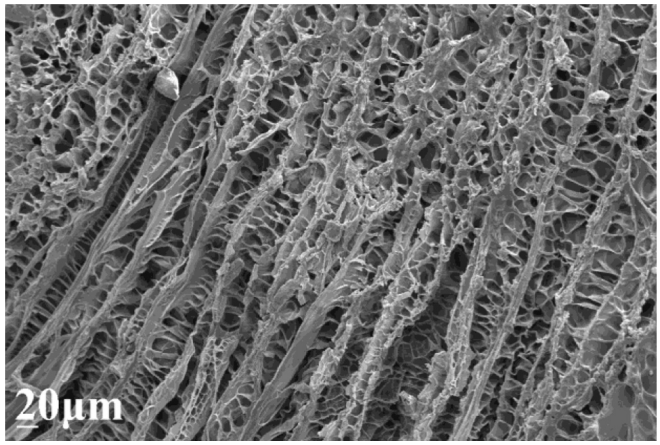

Fig. 1. Cross-sectional SEM image of pure PAAm-graft-chitosan matrix. The mass ratio of NMBA to AA is 0.06/10.

$$H_3PO_4 \text{ loading (wt\%)} = \frac{W_d - W_0}{W_d} \times 100\% \quad (1)$$

where W_d (g) was the mass of anhydrous H_3PO_4 imbibed PAAm-graft-chitosan membrane, W_0 (g) was the mass of dried PAAm-graft-chitosan membrane.

2.3. Electrochemical characterizations

The proton conductivity of the H_3PO_4 imbibed PAAm-graft-chitosan membranes in either hydrous or anhydrous state were characterized with ac-impedance spectroscopy using a CHI660E Electrochemical Workstation in a frequency range of 0.01 Hz–2 MHz and an ac amplitude of 10 mV in temperature range of 25–165 °C. Double coated PELCO Tabs™ carbon conductive tapes (TED PELLA, INC, 90% of polymer acrylic adhesive and 10% of carbon black) with a thickness of 0.1 mm were used as the electrodes. The ohmic resistance associated with the membrane was determined from high frequency intersection of the spectrum with the Z' axis, from which the proton conductivity can be calculated based on dimensional information.

Cyclic voltammetry (CV) was conducted at room temperature in 0.05 M H_3PO_4 aqueous solution using a three-compartment glass cell. The platinum wire with a diameter of 0.4 mm was pierced into a hydrated H_3PO_4 imbibed PAAm-graft-chitosan hydrogel which was used as working electrode. A platinum sheet and Ag/AgCl were used as counter electrode and reference electrode, respectively. Before the measurement, the electrolyte was deoxygenated by nitrogen bubbling for 5 min.

2.4. Membrane electrode assembly (MEA) and fuel cell tests

The gas diffusion electrodes (GDE, acquired from BASF Fuel Cell, Inc., formerly E-Tek, Inc.) with a platinum loading of 1.0 mg cm^{-2}, were used for this study. The MEA with an active area of 10 cm^2 was fabricated by hot-pressing a PAAM-graft-chitosan membrane between the two Kapton framed electrodes. The MEA was then assembled into a single cell fuel cell testing rig. The gas flow fields were made from graphite plates with single serpentine gas channels. Stainless steel end plates with attached heaters were used to clamp the graphite flow plates. A commercial fuel cell testing station (Fuel Cell Technology, Inc.) was used for fuel cell testing, while H_2 and pure oxygen were fed to the anode and cathode without any humidification, respectively. The instrument was controlled by home-programmed LabView Software (National Instruments, Austin, TX).

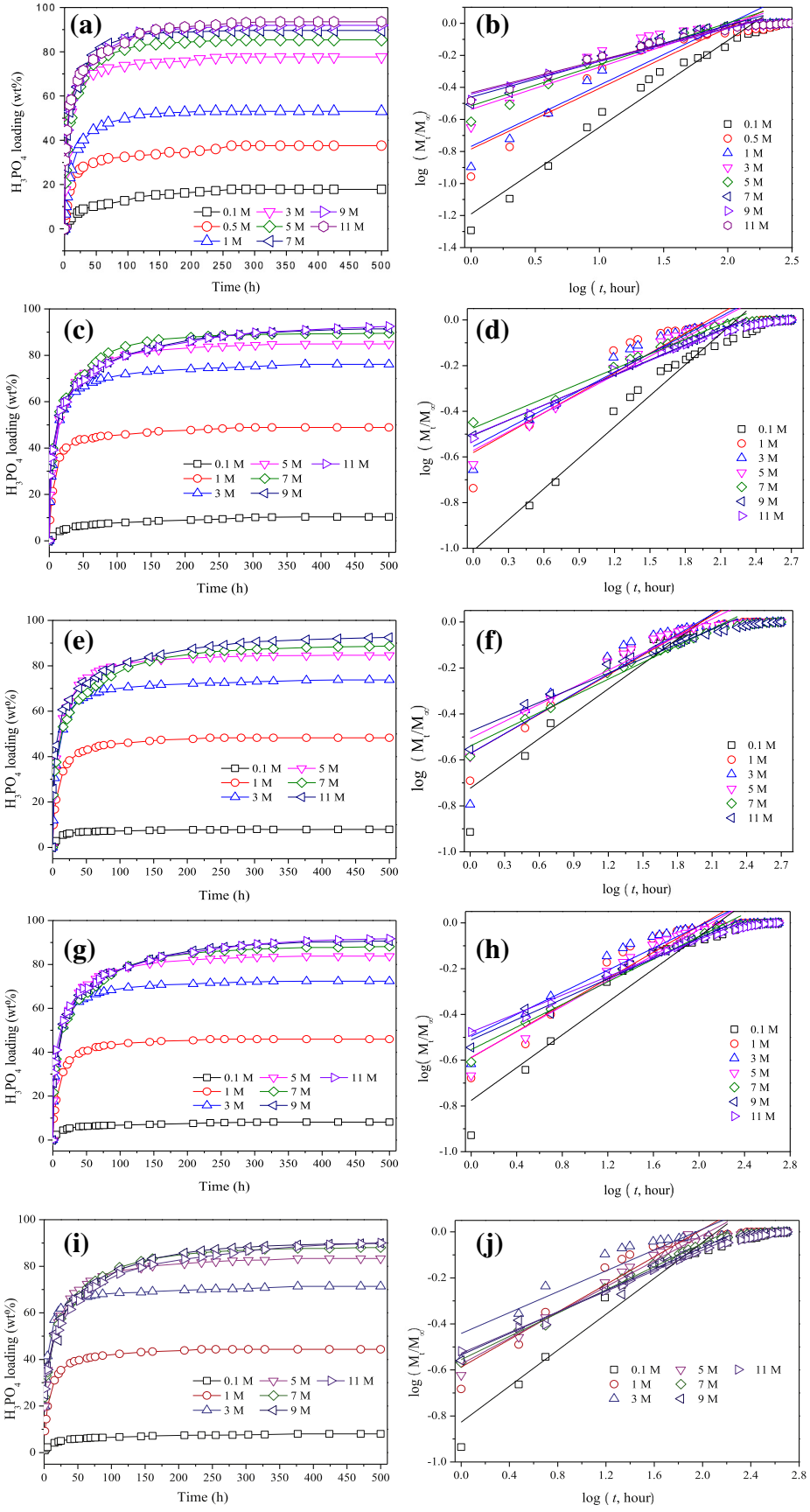

Fig. 2. Imbibition kinetics of PAAm-graft-chitosan membranes with NMBA/AAm ratios in various concentrations of H_3PO_4 aqueous solution: (a) & (b) 0.002/10 (g g^{-1}), (c) & (d) 0.004/10 (g g^{-1}), (e) & (f) 0.006/10 (g g^{-1}), (g) & (h) 0.008/10, and (i) & (j) 0.01/10 (g g^{-1}).

2.5. Other characterizations

The morphology was photographed with a Zeiss emission scanning electron microscopy (SEM). To observe the internal 3D microstructure of the PAAm-graft-chitosan membrane, a swollen PAAM-graft-chitosan hydrogel was freeze dried at a freezing temperature of around −60 °C for 72 h.

3. Results and discussion

3.1. Morphology observation

Fig. 1 shows the cross-sectional SEM image of PAAm-graft-chitosan matrix. The hydrogel matrix has a well-interconnected and microporous framework capable of caging enormous H_3PO_4 aqueous solution in its microporous structure during swelling process. The anhydrous H_3PO_4 can be sealed in the 3D framework during a dehydration process. In fact, the pore size and porosity can be controlled by adjusting synthesis conditions [22], such as crosslinker dosage, initiator dosage, reaction temperature, concentration of AAm monomer, and mass ratio of AAm to CS. The focus of the current work was to display the dependence of H_3PO_4 loading, proton conductivity and electrochemical performances of H_3PO_4 imbibed PAAm-graft-chitosan on NMBA dosage.

3.2. Imbibition kinetics

The imbibition kinetics of dense PAAm-graft-chitosan membranes in concentrated H_3PO_4 aqueous solutions, shown in Fig. 2, obeys the Flory theory from osmotic pressure across the PAAm-graft-chitosan membranes. The H_3PO_4 loading increases with imbibition time, indicating that it is a progressive diffusion of H_3PO_4 aqueous solution into 3D framework of PAAm-graft-chitosan matrix. An imbibition equilibrium can be obtained at an imbibition aging of around 15 days, and no further diffusion occurs under longer immersion time. In order to determine the nature of H_3PO_4 loading by PAAm-graft-chitosan, the accumulative H_3PO_4 loading over time have been fitted by the Fickian theory [23]:

$$\frac{W_t}{W_\infty} = kt^n \tag{2}$$

where W_t (g) and W_∞ (g) are the masses of the accumulative H_3PO_4 loading at time t and at equilibrium, respectively. K is a characteristic rate constant relating to the properties of PAAm-graft-chitosan matrix, and n is a transport number characterizing the transport mechanism. $n \leq 0.5$ reveals a Fickian or Case I transport behavior in which the PAAm-graft-chitosan framework relaxation is much faster than the diffusion; $n = 1$ gives a non-Fickian or Case II mode of transport where H_3PO_4 uptake is controlled by diffusion process. $0.5 < n < 1$ refers to an anomalous or a Case III mode in which structural relaxation is comparable to diffusion. By plotting $\log(W_t/W_\infty)$ versus $\log(t)$, n values are recorded and summarized in Table 1. The n values from the PAAm-graft-chitosan membrane at various NMBA/AAm ratios are all in the scale of 0–0.5, suggesting that it obeys a Fickian diffusion mechanism. There is a much higher contribution of molecular chain relaxation than diffusion of H_3PO_4 solution by osmotic pressure.

Table 1
Imbibition parameters of PAAm-graft-chitosan for H_3PO_4 aqueous solution.

NMBA/AAm ratio (g g^{-1})	Concentration of H_3PO_4 aqueous solution (M)							
	0.1	0.5	1	3	5	7	9	11
0.002/10	0.542	0.379	0.383	0.256	0.263	0.224	0.204	0.205
0.004/10	0.453	–	0.29	0.271	0.275	0.216	0.22	0.217
0.006/10	0.361	–	0.286	0.289	0.247	0.243	–	0.212
0.008/10	0.359	–	0.288	0.241	0.279	0.247	0.222	0.202
0.01/10	0.391	–	0.299	0.227	0.28	0.252	0.234	0.224

Fig. 3 shows the dependence of H_3PO_4 loading on NMBA dosage in H_3PO_4 imbibed PAAm-graft-chitosan. There is a diminishing dependence of H_3PO_4 loading on NMBA dosage, which is a reflection of microporous structure of PAAm-graft-chitosan matrix. It is believed that the synthesis of PAAm-graft-chitosan composite is a typical free-radical polymerization process, in which NMBA plays a role of 3D framework-making because of its macrobiradical nature. Therefore, increment of NMBA dosage gives an increasing crosslinking density, diminishing micropore structures, and therefore a H_3PO_4 loading [24].

3.3. Electrical characterization

The proton conductivity of H_3PO_4 imbibed PAAm-graft-chitosan membrane is of high dependence on NMBA dosage, as shown in Fig. 4. After systematic variation of NMBA dosage, we find that the dosage of NMBA at 0.06 wt% is an optimal condition in generating the highest proton conductivity.

Proton conductivity is one of the key parameters in evaluating H_3PO_4 imbibed PAAm-graft-chitosan membranes and is highly dependent on the H_3PO_4 loading. To explore higher H_3PO_4 loading and therefore better proton conductivity, anhydrous PAAm-graft-chitosan membranes are immersed into H_3PO_4 aqueous solution with concentrations scale of 0.1–11 M. The loading kinetics of H_3PO_4 is controlled by Flory theory [25]:

$$H_3PO_4 \text{ solution loading by PAAm} - \text{graft} - \text{chitosan PEM} = \frac{\left(\frac{i}{2V_u I^{1/2}}\right)^2 + \frac{1/2 - X_1}{V_1}}{V_e/V_0} \tag{3}$$

$$H_3PO_4 \text{ loading} = H_3PO_4 \text{ solution loading} \times H_3PO_4 \text{ concentration} \tag{4}$$

where i/V_u is the concentration of fixed charges referred to the anhydrous PAAm-graft-chitosan membrane, I is ionic strength in the H_3PO_4 aqueous solution, V_e/V_0 is crosslinking density of PAAm-

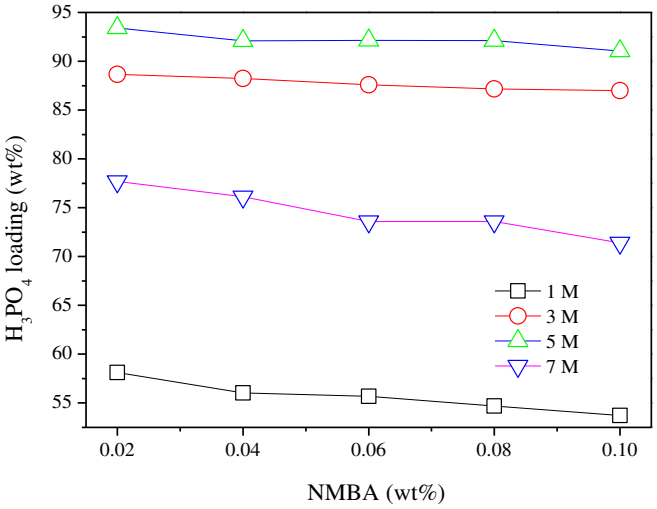

Fig. 3. H_3PO_4 loadings of the H_3PO_4 imbibed PAAm-graft-chitosan membranes as a function of NMBA dosage.

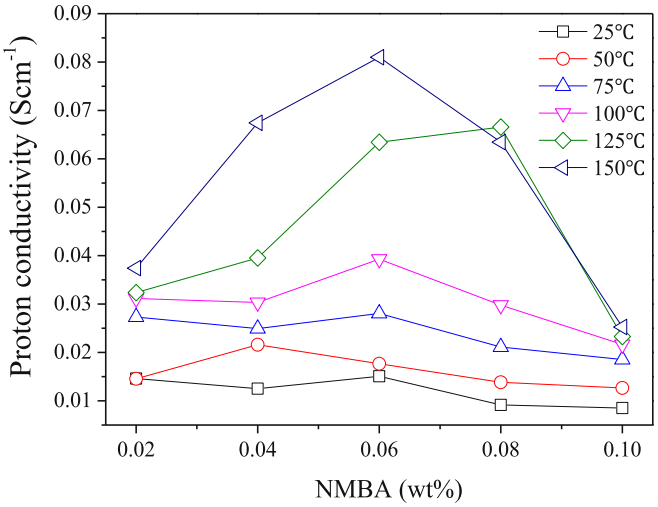

Fig. 4. Anhydrous proton conductivity of the H_3PO_4 imbibed PAAm-graft-chitosan membrane as a function of NMBA dosage.

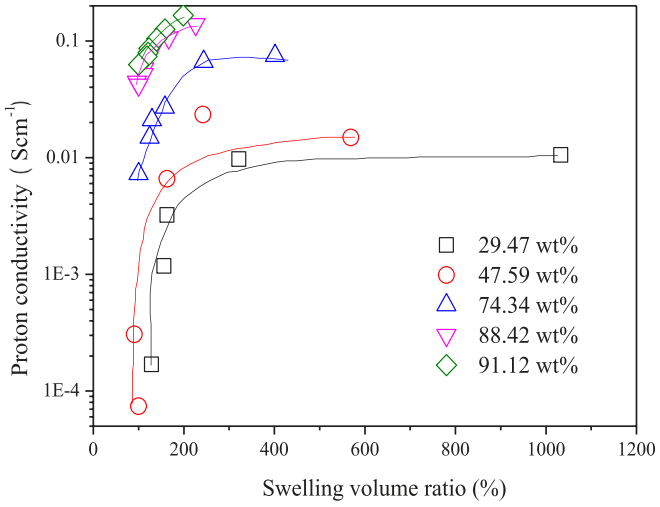

Fig. 6. Room-temperature proton conductivity of the hydrated H_3PO_4 imbibed PAAm-graft-chitosan membranes as a function of swelling volume ratio. The mass ratio of NMBA to AAm is 0.06/10.

graft-chitosan, and $(1/2 - X_1)/V_1$ is relative to solution affinity of PAAm-graft-chitosan. After systematic variation of concentration of H_3PO_4 aqueous solution, the increased H_3PO_4 loading in the target concentrations (Fig. 5) is highly expected to enhance anhydrous proton conductivity at room temperature. The highest H_3PO_4 loading of 96.63 wt% occurs at swelling in H_3PO_4 aqueous solution of 11 M, and therefore the highest room-temperature anhydrous proton conductivity of 0.058 S cm^{-1}.

There is an universality in hydrogel materials that the volume will be elevated by the filling of aqueous solution, therefore, swelling volume ratio (defined as $V_{swollen}/V_{dry}$) can be employed to evaluate the dependence of H_3PO_4 imbibed PAAm-graft-chitosan membranes on water content. Data on room-temperature proton conductivity from hydrated H_3PO_4 imbibed PAAm-graft-chitosan membranes are shown in Fig. 6. In the initial stage, the proton conductivity is elevated by two orders of magnitude compared with that at anhydrous state. Take 47.59 wt%H_3PO_4 imbibed PAAm-graft-chitosan membrane as an example, the anhydrous proton conductivity (conductivity at swelling volume ratio of 100%) is in the level of $\sim 10^{-5}$ S cm^{-1}, and it rushes up to $\sim 10^{-2}$ S cm^{-1} at swelling volume ratio of around 240%. With further increase in swelling volume ratio, the room-temperature conductivity reaches an equilibrium.

Hydrogen bondings between H_3PO_4 molecules and PAAm-graft-chitosan backbone as well as from H_3PO_4 molecules are believed as bridges for proton transport [26]. To record the formation of conducting bridges, anhydrous proton conductivities are plotted as a function of H_3PO_4 loading at room temperature (Fig. 7), giving a typical percolation effect like other conducting composites [27–29]. The point of abrupt increase in conductivity is always defined as percolation threshold. From Fig. 7, one can see that conductivity percolation occurs at around 65 wt%H_3PO_4 loading, indicating that the conducting channels from hydrogen-bridges of H_3PO_4 are interconnected at 65 wt%H_3PO_4. For example, the anhydrous conductivity is in the level of $\sim 10^{-6}$ S cm^{-1} at H_3PO_4 loading of 29.47 wt%, and it increases to 5.96×10^{-4} S cm^{-1} at 62.68 wt%H_3PO_4.

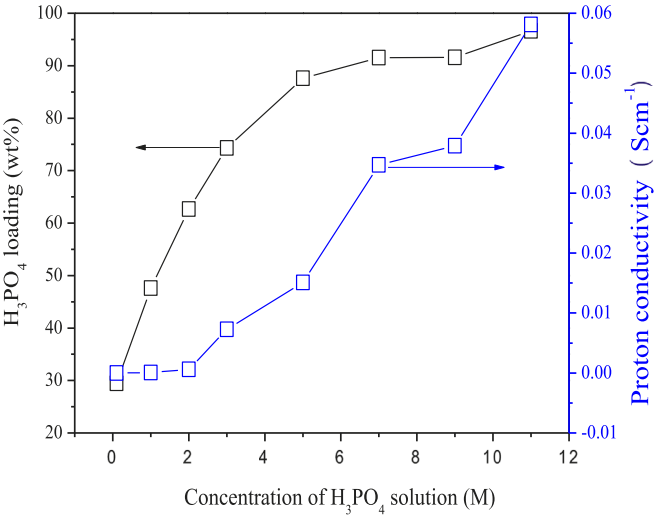

Fig. 5. Anhydrous proton conductivity and H_3PO_4 loading of the H_3PO_4 imbibed PAAm-graft-chitosan membrane as a function of H_3PO_4 concentration at fully hydrated equilibrium state. The measurement was carried out at room temperature. The mass ratio of NMBA to AAm is 0.06/10.

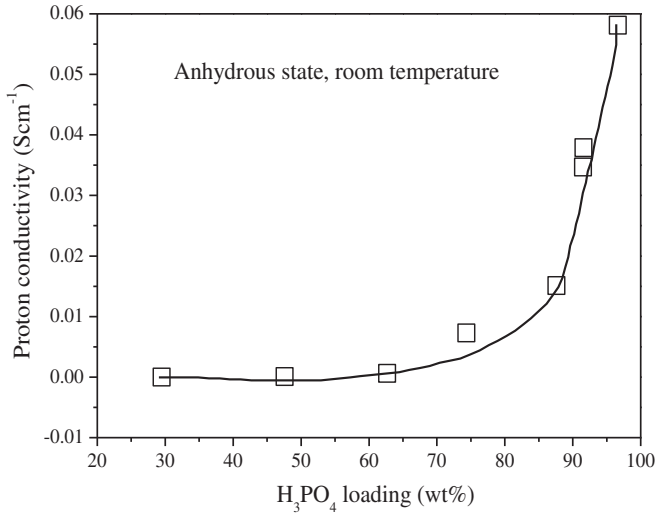

Fig. 7. Room-temperature anhydrous conductivity percolation effect of H_3PO_4 imbibed PAAm-graft-chitosan membranes. The mass ratio of NMBA to AAm is 0.06/10.

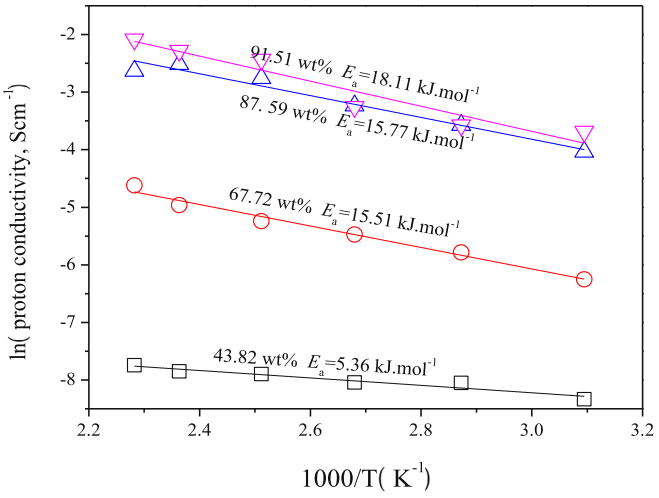

Fig. 8. Arrhenius plots of H_3PO_4 imbibed PAAm-graft-chitosan membranes measured in anhydrous conditions. The mass ratio of NMBA to AAm is 0.06/10.

The anhydrous proton conductivity from H_3PO_4 imbibed PAAm-graft-chitosan membranes measured from 25 to 165 °C follows an Arrhenius relationship well, as is shown in Fig. 8. A proton conductivity as high as 0.13 S cm^{-1} is recorded at 91.51 wt%H_3PO_4 imbibed PAAm-graft-chitosan membrane at 165 °C. Interestingly, the activation energy, E_a, systematically increases with H_3PO_4 loading, which is opposite to that of H_3PO_4 doped PBI membranes and other conducting composite system [30], but is consistent with our previous reports and other system on PAM/H_3PO_4 membranes [13–17,31]. E_a is closer to that of pure H_3PO_4 (23.05 kJ mol^{-1}) at higher H_3PO_4 loading. Lower E_a values in H_3PO_4 imbibed PAAm-graft-chitosan membranes suggest a facile proton transport along the conducting channels. It is reasonable that the conducting channels tend to be interconnected at higher H_3PO_4 loading, whereas the conducting regions are isolated at lower H_3PO_4 loading.

91.49 wt%H_3PO_4 imbibed PAAm-graft-chitosan membrane is employed to evaluate the anhydrous proton conductivity stability at 130 °C, as is shown in Fig. 9. Over a 12 h period, more than 100% of the initial proton conductivity is preserved at 130 °C, suggesting

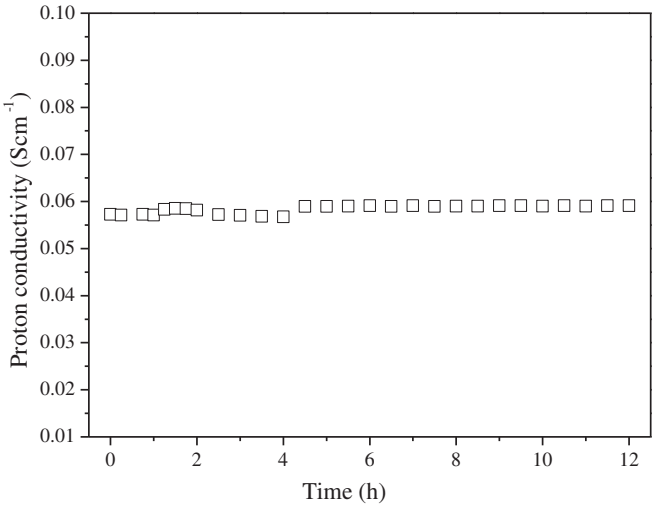

Fig. 9. Stability of anhydrous proton conductivity for 91.49 wt%H_3PO_4 imbibed PAAm-graft-chitosan membrane measured at 130 °C.

that it is a good high-temperature PEM candidate for potential PEMFC applications.

3.4. Electrochemical characterizations

3D PAAm-graft-chitosan hydrogel material not only imbibes enormous H_3PO_4, but also provides interconnecting channels for proton transport. Microporous structure can be apparently observed from the SEM morphology. To determine the unobstructed transport of protons within the micropores, CV measurements are carried out by piercing a platinum wire into a hydrated H_3PO_4 imbibed PAAm-graft-chitosan hydrogel membrane which is used as working electrode. A platinum sheet is employed as a counter electrode accompanied with an Ag/AgCl reference electrode. The electrolyte is H_3PO_4 aqueous solution with the same concentration to that for swelling of PAAm-graft-chitosan. Fig. 10a–e shows the CV plots obtained from 0.05 M H_3PO_4 solution imbibed PAAm-graft-chitosan hydrogel. A typical hydrogen desorption peak area appears at the potential range of −0.3–0 V because of the oxidation reaction $H_2 - 2e \rightarrow 2H^+$. In the reduction scan, all the CVs show a peak at around 0.3 V, corresponding to the reduction of surface oxides on Pt wires. The distinctive feature in this peak is that the position of peak shifted toward lower potential. A hydrogen adsorption peak is recorded in the potential region of −0.3 ~ −0.1 V attributed to the reduction of protons ($2H^+ + 2e \rightarrow H_2$). These results can be employed to detect the proton transport in hydrated H_3PO_4 imbibed PAAm-graft-chitosan membranes. By plotting the peak current of hydrogen adsorption versus square root of scan rate, as shown in Fig. 10f, we can quantify the intrinsic relations of proton transport in the hydrated H_3PO_4 imbibed PAAm-graft-chitosan membranes. One can see that the membrane scanned at higher scan rate has considerable higher reduction peak current than those at lower ones. The increased peak current values suggest a large surface area and fast reaction rate, which makes the PEMs robust in transferring protons within the interconnecting channels. Furthermore, we can conclude that the proton transfer is dominated by the diffusion of counterions in the PEMs, such as $H_2PO_4^-$, HPO_4^{2-}, PO_4^{3-}.

CV curves of 20 cycles have been scanned to determine the continuous transport of protons within H_3PO_4 imbibed PAAm-graft-chitosan membranes, as is shown in Fig. 11. No apparent decrease in peak current density from hydrogen adsorption is observed, indicating that the 3D interconnected framework of PAAm-graft-chitosan serves as superhighways in transferring protons, which is desirable for efficient PEMFCs.

3.5. Fuel cell performance

A PAAm-graft-chitosan membrane with a thickness of around 500 μm was eventually assembled into a fuel cell for performance evaluation. Detailed description of fuel cell assembly can be found in the Experimental Section. The *V–I* and *P–I* characteristics measured at 150 °C with dry H_2 as the fuel and dry oxygen as the oxidant are shown in Fig. 12. A maximum power density of 405 mW cm^{-2} @ 0.81 A cm^{-2} was achieved at 150 °C. While the demonstrated performance is lower compared to H_3PO_4-doped PBI [32], the overall performance is satisfactory and comparable to other proposed PEMFCs [33], considering the fact that both membrane and electrode were not optimized.

4. Conclusions

In summary, H_3PO_4 imbibed PAAm-graft-chitosan PEMs have been successfully fabricated using the imbibition of PAAm-graft-chitosan superabsorbents toward H_3PO_4 aqueous solution. The 3D

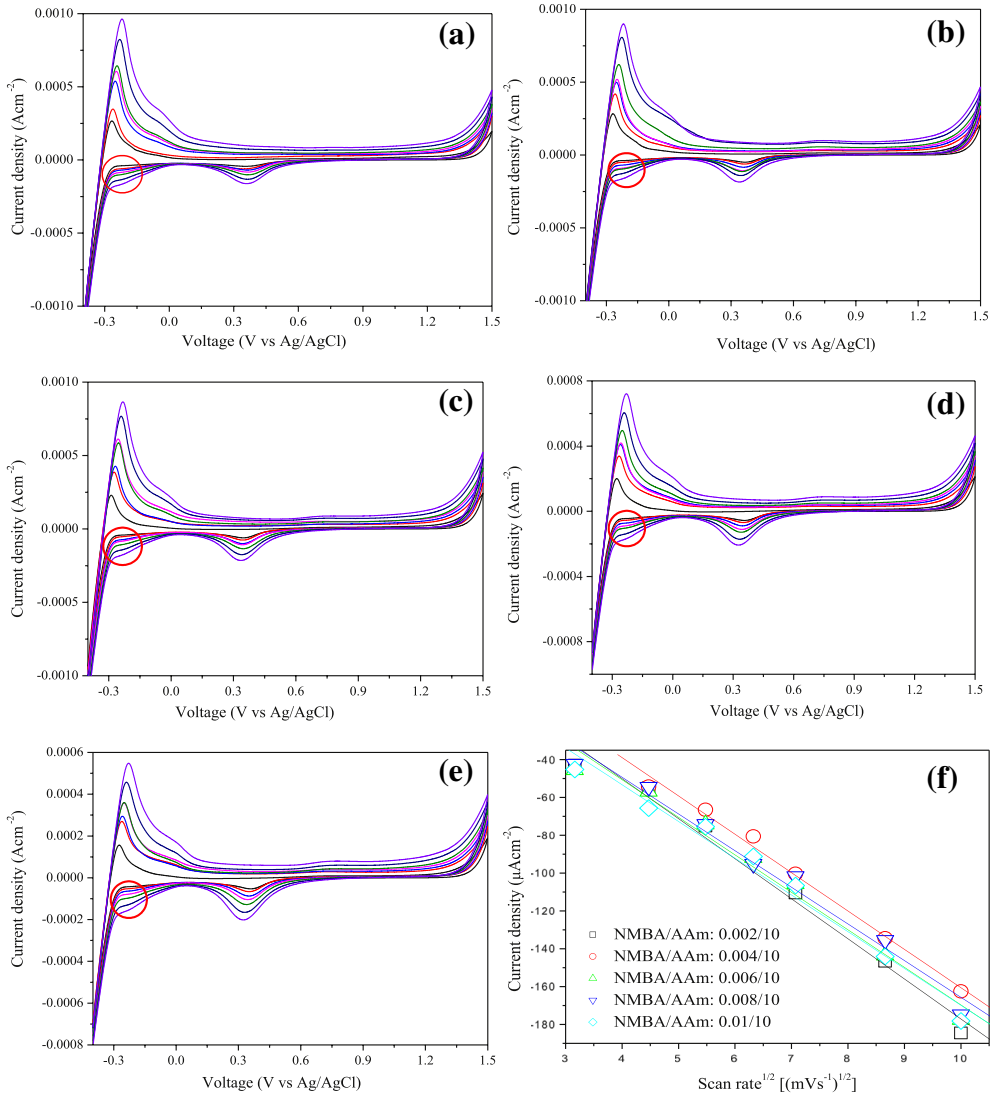

Fig. 10. CV curves recorded in 0.05 M H_3PO_4 aqueous solution imbibed PAAm-graft-chitosan hydrogel at various NMBA/AAm ratios: (a) 0.002/10, (b) 0.004/10, (c) 0.006/10, (d) 0.008/10, and (e) 0.01/10. From inner to outer: 10, 20, 30, 40, 50, 75, and 100 mV·s^{-1}. (f) Linear relationships of peak current density as a function of scan rate$^{1/2}$.

interconnected microporous structure provides placeholder for H_3PO_4 storage. The protons transfer by a Grottuss mechanism, migrating across hydrogen bonds present in H_3PO_4 as well as those formed between H_3PO_4 molecules and functional groups in PAAm-graft-chitosan matrix. Results indicate that there is a facile proton transfer along the hydrogen bonding between H_3PO_4 molecules and PAAm-graft-chitosan in comparison with that from H_3PO_4 themselves. A promising anhydrous proton conductivity of 0.13 S cm^{-1} is recorded at 165 °C because of considerable H_3PO_4 loading. Resultant H_3PO_4 imbibed PAAm-graft-chitosan

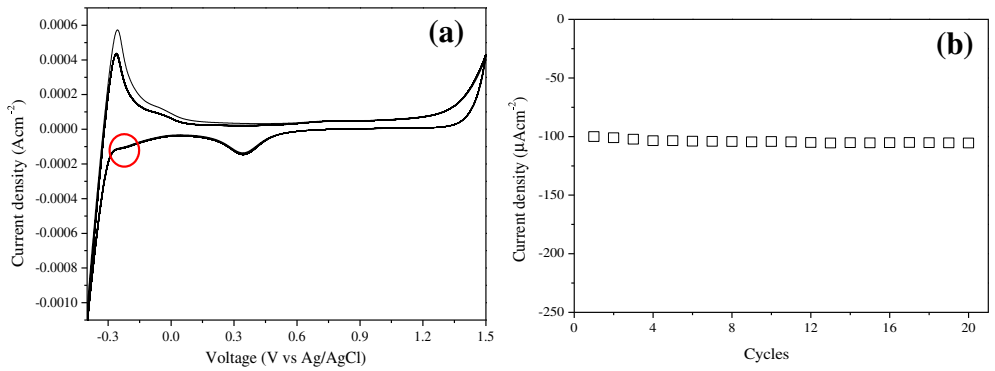

Fig. 11. (a) CV curves recorded in 0.05 M H_3PO_4 aqueous solution imbibed PAAm-graft-chitosan hydrogel at NMBA/AAm ratio of 0.006/10 and scan rate of 50 mV·s^{-1}. (b) Peak current densities as a function of cycles.

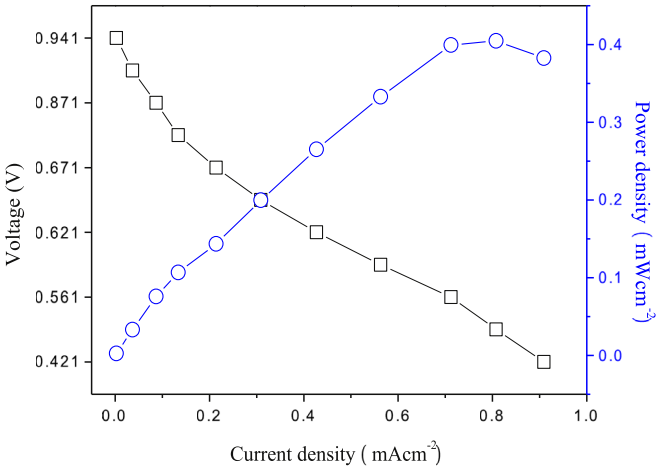

Fig. 12. V–I and P–I characteristics of 91.49 wt%H_3PO_4 imbibed PAAm-graft-chitosan membrane at 150 °C under anhydrous conditions. Gas stream: H_2/O_2, 135 °C; gas flow rates: H_2 1.2 stoich, O_2 2 stoich.

membranes show excellent stability in proton conductivity and proton transfer. A fuel cell using a thick membrane as a PEM showed a peak power density of 405 mW cm^{-2} with O_2 and H_2 as the oxidant and fuel, respectively. These attributes demonstrate the H_3PO_4 imbibed PAAm-graft-chitosan to be a viable high-temperature PEM. These profound advantages along with low-cost synthesis, impressed proton conductivity, good stability, and scalable matrix and proton conductors promise the new materials to be strong alternatives as high-temperature PEMs.

Acknowledgments

The authors gratefully acknowledge Ocean University of China for providing Seed Fund to this project, and Fundamental Research Funds for the Central Universities (201313001, 201312005), Shandong Provincial Natural Science Foundation (ZR2011BQ017), Research Project for the Application Foundation in Qingdao (13-1-4-198-jch), and National Natural Science Foundation of China (61366003).

References

[1] M. Unlu, J.F. Zhou, P.A. Kohl, Angew. Chem. Int. Ed. 49 (2010) 1299–1301.
[2] G. Chamoulaud, D. Belanger, Langmuir 20 (2004) 4989–4995.
[3] S.J. Peighambbardoust, S. Rowshanzamir, M. Amjadi, Int. J. Hydrogen Energy 35 (2010) 9349–9384.
[4] C.H. Shen, S.L. Hsu, E. Bulycheva, N. Belomoina, J. Mater. Chem. 22 (2012) 19269–19275.
[5] R. Devanathan, Energy Environ. Sci. 1 (2008) 101–119.
[6] Y.L. Chen, Y.Z. Meng, A.S. Hay, Macromolecules 38 (2005) 3564–3566.
[7] Z.Q. Shi, S. Holdcroft, Macromolecules 38 (2005) 4193–4201.
[8] E.P. Jutemar, S. Takamuku, P. Jannasch, Polym. Chem. 2 (2011) 181–191.
[9] J.L. Lu, H.L. Tang, C.W. Xu, S.P. Jiang, J. Mater. Chem. 22 (2012) 5810–5819.
[10] V.D. Noto, E. Negro, J.Y. Sanchez, C. Iojoiu, J. Am. Chem. Soc. 132 (2010) 2183–2195.
[11] H.W. Zhang, P.K. Shen, Chem. Rev. 112 (2012) 2780–2832.
[12] J.A. Asensio, E.M. Sanchez, P. Gomez-Romero, Chem. Soc. Rev. 39 (2010) 3210–3239.
[13] Q.W. Tang, H.Y. Cai, S.S. Yuan, X. Wang, W.Q. Yuan, Int. J. Hydrogen Energy 38 (2013) 1016–1026.
[14] Q.W. Tang, S.S. Yuan, H.Y. Cai, J. Mater. Chem. A 1 (2013) 630–636.
[15] Q.W. Tang, G.Q. Qian, K. Huang, RSC Adv. 2 (2012) 10238–10244.
[16] Q.W. Tang, K. Huang, G.Q. Qian, B.C. Benicewicz, J. Power Sources 229 (2013) 36–41.
[17] Q.W. Tang, G.Q. Qian, K. Huang, RSC Adv. 3 (2013) 3520–3525.
[18] J.M. Lin, Q.W. Tang, D. Hu, X.M. Sun, Q.H. Li, J.H. Wu, Colloids Surf. A 346 (2009) 177–183.
[19] Q.W. Tang, J.H. Wu, J.M. Lin, Q.H. Li, S.J. Fan, J. Mater. Sci. 43 (2008) 5884–5890.
[20] Q.W. Tang, X.M. Sun, Q.H. Li, J.H. Wu, J.M. Lin, Sci. Technol. Adv. Mater. 10 (2009) 015002.
[21] C.J. Zhou, Q.L. Wu, Colloids Surf. B 84 (2011) 155–162.
[22] J.H. Wu, Y.L. Wei, J.M. Lin, S.B. Lin, Polymer 44 (2003) 6513–6520.
[23] N.W. Franson, N.A. Peppas, J. Appl. Polym. Sci. 28 (1983) 1299–1310.
[24] J.P. Zhang, Q. Wang, A.Q. Wang, Carbohydr. Polym. 68 (2007) 367–374.
[25] P.J. Flory, Principles of Polymer Chemistry, Cornel University Press, New York, 1953.
[26] S.M. Haile, P.N. Pintauro, J. Mater. Chem. 20 (2010) 6211–6213.
[27] J. Obrzut, J.F. Douglas, O. Kirllov, F. Sharifi, J.A. Liddle, Langmuir 29 (2013) 9010–9015.
[28] B. Mayoral, P.R. Hornsby, T. McNally, T.L. Schiller, K. Jack, D.J. Martin, RSC Adv. 3 (2013) 5162–5183.
[29] Q.W. Tang, X.M. Sun, Q.H. Li, J.M. Lin, J.H. Wu, J. Mater. Sci. 44 (2009) 849–854.
[30] Q.F. Li, J.O. Jensen, R.F. Savinell, N.J. Bjerrum, Prog. Polym. Sci. 34 (2009) 449–477.
[31] W. Wieczorek, J.R. Stevens, Polymer 38 (1997) 2057–2065.
[32] Y. Zhai, H. Zhang, D. Xing, Z. Shao, J. Power Sources 164 (2007) 126–133.
[33] M. Georgezi, V. Deimede, N. Gourdoupi, N. Triantafyllopoulos, S. Neophytides, J.K. Kallitsis, Macromolecules 41 (2008) 9051–9056.